Substrate Dependence of Self-Assembly of Alkanethiol: X-ray Absorption Fine Structure Study

H. Kondoh, A. Nambu, Y. Ehara, F. Matsui,† T. Yokoyama,‡ and T. Ohta*

Department of Chemistry, Graduate School of Science, The University of Tokyo Hongo, Tokyo 113-0033, Japan

Received: April 24, 2004; In Final Form: June 4, 2004

We have investigated effects of substrates on self-assembly of alkanethiol molecules by means of X-ray absorption fine structure spectroscopy. Molecular orientation of hexanethiolate adsorbed on various substrates such as Cu(111), Ag(111), Ag(100), Si(111), and their oxygen-covered surfaces has been explored by C K-edge and S K-edge near-edge X-ray absorption fine structure (NEXAFS). It was revealed that the alkyl-chain orientation is not correlated to the S−C bond orientation but primarily determined by the molecular density that definitely depends on the substrate surface. Precovered oxygen overlayers do not prevent thiol molecules from being adsorbed but promote their adsorption rate. The surface oxygen atoms are removed via formation and desorption of H_2O. The interface structure of a hexanethiolate monolayer on O/Cu(100) has been studied in detail by use of S K-edge surface extended X-ray absorption fine structure (SEXAFS). The SEXAFS results indicated that hexanethiol adsorption induces a lateral displacement of surface Cu atoms toward the sulfur atom of the thiolate with a concomitant breaking of the −O−Cu−O− one-dimensional chain.

I. Introduction

Self-assembly of molecules is strongly influenced by physical and chemical environments where the self-assembly takes place. Particularly, in self-assembled monolayers (SAMs), solid substrates do not only serve as supports but also play a decisive role to the self-assembly. So far, alkanethiol SAMs on Au(111) have been extensively studied as a prototypical SAM system because they are simple and quite easy to prepare and have highly ordered structures.[1−4] However, the number of the studies on alkanethiol SAMs on other substrates has been relatively limited.[4]

The structure of alkanethiolate SAMs on Ag surfaces prepared by the immersion method has been studied with scanning tunneling microscopy (STM),[5] low-energy atom diffraction (LEAD),[6] infrared reflection absorption spectroscopy (IRAS),[7] and near-edge X-ray absorption fine structure (NEXAFS).[8] The STM and LEAD studies showed clear evidence for an incommensurate structure with respect to the (111) surface of Ag. Both the IRAS and NEXAFS studies indicated that the alkyl chains in the SAMs on Ag substrates are aligned almost vertically with a tilt angle smaller than that on Au(111). Since these SAMs were prepared under atmospheric condition, the Ag surfaces were covered by adsorbed oxygen prior to the formation of the SAMs. In alkanethiolate monolayer on a clean Ag(100) surface prepared by the vacuum deposition method, however, the thiolate molecules have no ordered structure and the alkyl chains are significantly inclined to the surface.[9] On the other hand, in clean Cu surfaces, vacuum-deposited hexanethiol molecules form well-ordered SAMs both on Cu(111) and Cu(100).[10−12] However, it is unclear how precovered oxygen atoms affect the formation of the SAMs. Furthermore, adsorption structures of alkanethiol adsorbed on semiconductor surfaces have not been well understood though they are important for a wide variety of technological applications such as molecular electronic devices.

Recently, Zharnikov and co-workers have reported the relation between the molecular orientation and the molecule−substrate interface structure for alkanethiol derivative SAMs on Au and Ag substrates.[13] On the basis of the substrate-dependent change of the alkyl-chain orientation, they proposed that the molecular alignment in the thiolate SAMs is strongly influenced by the S−C bond angle that is primarily determined by the thiolate−substrate interactions. However, they did not measure the S−C bond angles directly but deduced them by the even−odd effect of the alkyl-carbon number on the orientation of the terminal methyl group. More direct structural studies on the orientations of the alkyl chains and the S−C bonds are needed to clarify the correlation. Systematic comparison of the adsorption structure of alkanethiolate on various substrate surfaces such as clean and oxygen-precovered coinage metal surfaces and semiconductor surfaces will shed light on the role of molecule−substrate interactions on the molecular self-assembly.

In this study, we measured both C−K NEXAFS and S−K NEXAFS spectra for monolayers of hexanethiolate (hereafter denoted by C6-thiolate), which is one of the most thoroughly studied alkanethiolates, self-assembled on various substrate surfaces, Cu(111), O/Cu(111), Ag(100), O/Ag(111), and O/Ag-(100), and compared their alkyl-chain alignments with the corresponding S−C bond orientations to understand the substrate effects on the structure of the alkanethiolate SAMs. For comparison, we have also conducted C K−NEXAFS experiments for C6-thiolate and C1-thiolate monolayers formed on Si(111)-7 × 7 surfaces which have dangling bonds. Furthermore, to clarify how the precovered oxygen atoms affect the adsorption structure of thiolate, the local geometry around the sulfur atom of the thiolate adsorbed on an oxygen-saturated Cu(100) surface

* Corresponding author. Tel: +81-3-5841-4331; fax: +81-3-3812-1896; e-mail address: ohta@chem.s.u-tokyo.ac.jp.

† Present address: Nara Advanced Institute of Science and Technology, Nara 630-0192, Japan.

‡ Present address: Institute of Molecular Science, Okazaki 444-8585, Japan.

10.1021/jp048208k CCC: $27.50
Published on Web 07/16/2004

with a $(2\sqrt{2} \times \sqrt{2})$R45° structure was studied with S K-edge surface extended X-ray absorption fine structure (SEXAFS). From a systematic comparison of these results, we discuss the role of the substrate surface on the self-assembly.

II. Experimental Section

The experiments were performed in two separate ultrahigh vacuum (UHV) chambers with base pressures less than 1×10^{-10} Torr. Cu(111) and Cu(100) surfaces were mechanically polished with 5, 1, 0.3, and 0.05 μm alumina powder stepwise to obtain a mirror finished plane and electrochemically etched in a methanol solution of nitric acid. Ag(111) and Ag(100) surfaces were mechanically polished in the same manner, followed by chemical etching by alternate dipping into an aqueous solution of 10 wt % H_2O_2 and 1 wt % NaCN and a 3.6 wt % NaCN aqueous solution. Si(111) wafers were etched by the standard Shiraki method.[14] The Cu and Ag surfaces were cleaned by repeated cycles of Ar ion sputtering and annealing. Residual carbon species on Cu(111) were removed by the O_2 treatment (sample temperature: 350 °C, ambient O_2 pressure: 5×10^{-7} Torr). The Si(111) surface was first degassed by resistive heating at 800 K for several hours and then annealed at 1000 K for a few minutes. Clean Si(111)-7 × 7 surfaces were obtained by flash annealing to 1400 K for 30 s. The cleanliness and ordering of these surfaces were confirmed by XAFS and LEED.

C6-thiolate monolayers were prepared by exposing the Cu, Ag, and Si surfaces to gaseous hexanethiol (hereafter denoted by C6-thiol) introduced via a variable leak valve at room temperature.[15] Oxygen-covered Cu(111) and Cu(100) surfaces were formed by dissociative adsorption of gaseous O_2 under UHV condition. These oxygen-covered Cu surfaces were exposed to gaseous C6-thiol to form C6-thiolate monolayers. Oxygen-covered Ag(111) and Ag(100) surfaces were prepared by brief exposure (30 s) of clean surfaces to air at room temperature. Then, the oxygen-covered Ag surfaces were dipped into 1 mM ethanolic solution of C6-thiol for 48 h. After dipping, the surfaces were rinsed with pure ethanol several times and introduced into the UHV chambers.

C K-edge NEXAFS (280−340 eV) measurements were carried out at the plane-grating monochromator beamline BL-7A[16] of the Photon Factory (KEK−PF, Tsukuba). Spectra were taken with the partial electron yield mode using a microchannel plate (MCP) with a retarding voltage of −200 eV. The typical energy resolution was 0.5 eV around the C K-edge region. Coverages of the surface thiolates were deduced from the edge jump of C−K NEXAFS spectra by calibrating to that of a C6-thiolate-saturated Au(111) surface whose molecular density is 21.6 Å^2/molecule.[1]

S K-edge NEXAFS (2460−2510 eV) and SEXAFS (2400−3000 eV) measurements were performed at the double-crystal monochromator station BL-11B[17] of the Photon Factory by the fluorescence yield method using a UHV-compatible gas-flow proportional counter with P10 gas (10% CH_4 in Ar). A Ge(111) crystal pair was used as the monochromator, whose energy resolution around the S K-edge region was ∼1.5 eV. The S K-edge XAFS spectra were measured with different incidence angles to obtain information on the local structure around the sulfur atom. All the S−K XAFS spectra were taken at a sample temperature of 130 K.

III. Results

A. C K-Edge NEXAFS. *Cu and O/Cu Surfaces.* Figure 1a shows polarization dependence of C K-edge NEXAFS spectra for C6-thiol adsorbed on Cu(111) at room temperature with various exposures. At 40 langmuirs (1 langmuir = 1×10^{-6} Torr sec), two prominent peaks are observed at 288 and 292.5 eV. These peaks are attributed to excitations of the C 1s electron to a σ^*(C−H) + Rydberg state and a σ^*(C−C) resonance, respectively. The transition moment of the former excitation orients perpendicular to the −C−C−C− plane, while that of the latter one lies along the −C−C−C− molecular axis.[18] According to these assignments, the polarization dependence observed for 40 langmuirs, where the σ^*(C−C) resonance is most enhanced at the grazing incidence, clearly shows that the molecular axes of the C6-thiolates stand upright on the surface. On the other hand, at the lowest exposure (13 langmuirs), the polarization dependence is reversed, indicating that the molecular axes are lying down on the surface. At an intermediate exposure of 22 langmuirs, the polarization dependence vanishes, suggesting a tilted orientation with a large angular distribution. Such a change in molecular orientation with exposure has been observed for other alkanethiolate SAM systems on Au(111)[19,20] and Cu(100).[11]

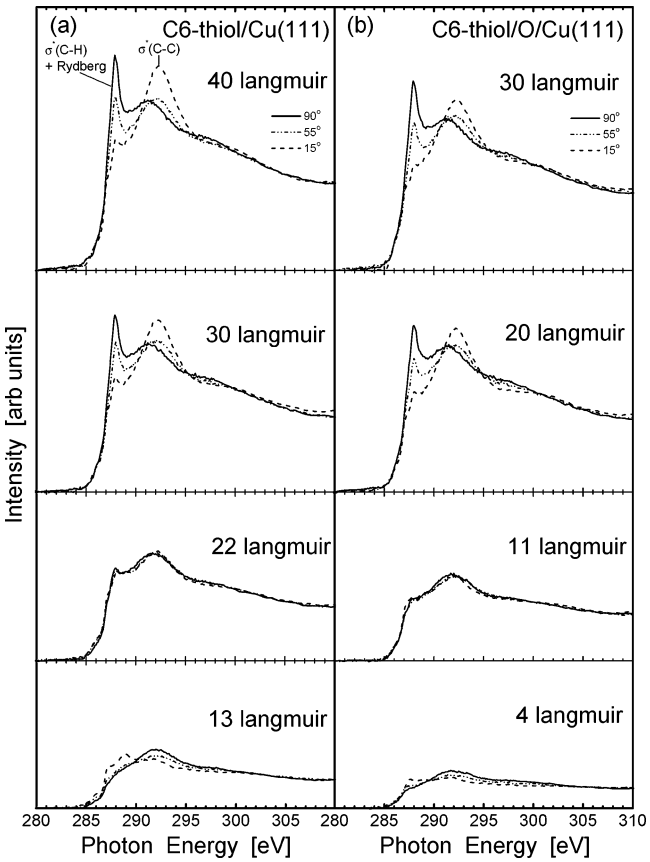

Figure 1. C K-edge NEXAFS spectra of hexanethiolate (C6-thiolate) monolayers adsorbed on a clean Cu(111) (a) and an oxygen-precovered Cu(111) (b) surfaces. The precovered oxygen coverage was 0.5 ML, saturated at room temperature. The clean and oxygen-precovered Cu(111) surfaces were exposed to gaseous hexanethiol (C6-thiol) with various exposures at room temperature. Two prominent peaks are observed at 288 and 292.5 eV, which are assigned to excitations from C 1s to a σ^*(C−H) + Rydberg state and a σ^*(C−C) state, respectively. Polarization dependence of the spectra was monitored with three X-ray incident angles (90°, 55°, and 15°) from the surface parallel.

In Figure 1b are shown C K-edge NEXAFS spectra for C6-thiol adsorbed on an oxygen-saturated Cu(111) surface at room temperature. The O-saturated Cu(111) surface showed a complex structure with an oxygen coverage of 0.5 ML, which is similar to the (111) plane of Cu_2O and has been regarded as an oxide precursor to bulk oxide phases.[21] This surface was exposed

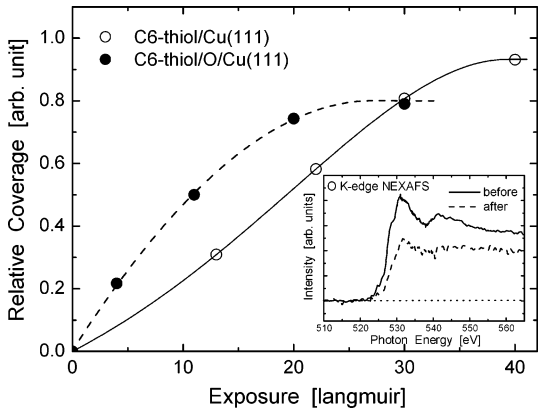

Figure 2. Uptake curves of C6-thiolate on the clean (open circles) and the oxygen-saturated (solid circles) Cu(111) surfaces as a function of exposure. Inset: O K-edge NEXAFS spectra taken before (solid line) and after (dashed line) the saturation of C6-thiolate on the oxygen-precovered Cu(111) surface.

to gaseous C6-thiol at room temperature. Interestingly, C6-thiol molecules readily adsorb on the oxygen-saturated surface in the same manner as seen for the clean surface; at a low exposure C6-thiol molecules adsorb with a lying-down configuration, whereas they stand up at higher exposures. Comparison of uptake curves between clean and oxygen-saturated Cu(111) surfaces, however, reveals that precovered oxygen atoms promote the adsorption rate of the thiol as shown in Figure 2. Arriving thiol molecules are more easily adsorbed on the surface in the presence of oxygen because of hydrogen abstraction from the SH group by the preadsobed oxygen atom leading to facile formation of Cu−thiolate covalent bond. Alkanethiol SAMs were first prepared by the immersion method 45 years ago on Cu condenser plates in steam engines, whose surface must have been covered by thick oxides.[22] This suggests that Cu oxide films have a strong affinity for alkanethiol molecules. Surface oxygen atoms that work as a hydrogen abstracter desorb from the surface in the form of water as evidenced by a decrease in oxygen coverage after the thiolate-SAM formation (inset of Figure 2). The inset shows O K-edge NEXAFS spectra taken before and after the SAM formation on the O(0.5 ML)/Cu(111) surface. Obviously, a part of oxygen atoms are removed from the surface by the SAM formation. The decrease in oxygen coverage is estimated from the edge-jump change to be 0.14 ML, which is just half of the surface thiolate coverage (0.28 ML). This suggests that the thiol molecules adsorb on the O-covered surface according to the reaction scheme

$$2C_6H_{13}SH_g + O_a \rightarrow 2C_6H_{13}S_a + H_2O_g\uparrow$$

To estimate the orientation angle of the alkyl chains in the saturated monolayer, the C K−NEXAFS spectra for that on Cu(111) were curve-fitted by summation of a step function and symmetric and asymmetric Gaussian functions as shown in Figure 3. In the preedge region, at least three components were needed to reproduce the experimental curves, being consistent with previous theoretical and experimental works[23,24] on saturated hydrocarbons. Since the preedge region is complicated, the orientation angle was deduced from the polarization dependence of the σ^*(C−C) peak at 292.5 eV, which results in 30 ± 5° from the surface normal. The same analysis was performed for the saturated monolayer on O/Cu(111) and yields 38 ± 5° from the surface normal.

Ag and O/Ag Surfaces. Figure 4 shows polarization dependence of C K-edge NEXAFS spectra taken for C6-thiol adsorbed

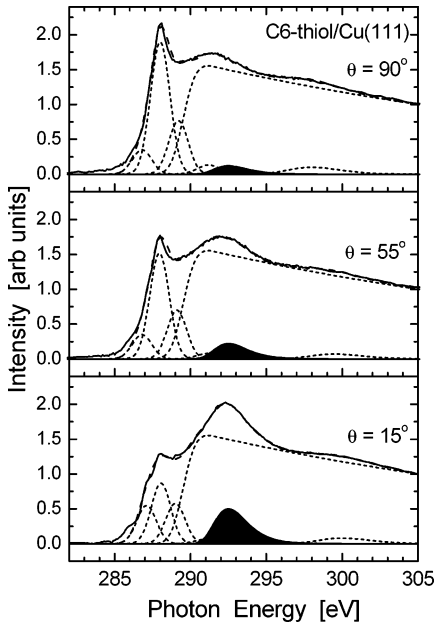

Figure 3. An example of curve-fitting analyses of the C K-edge NEXAFS spectra. Three symmetric Gaussian functions and three asymmetric Gaussian functions were used for the preedge region and the postedge region, respectively, in addition to a step function. To estimate the orientation angle of the alkyl chain, the intensity of the σ^*(C−C) resonance peak observed at 292.5 eV (filled by black color) was used for the polarization dependence analysis.

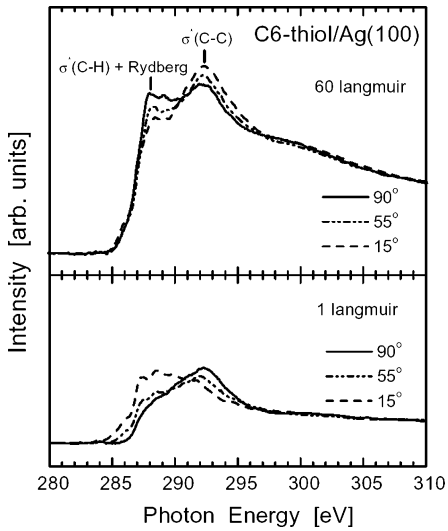

Figure 4. C K-edge NEXAFS spectra of C6-thiolate monolayers adsorbed on a clean Ag(100) surface with exposures of 60 (upper) and 1 (lower) langmuirs at room temperature. Higher exposures more than 60 langmuirs of C6-thiol induced no increase in coverage.

on a Ag(100) surface with a low and a high exposures at room temperature. At the low exposure (1 langmuir), adsorbed C6-thiolate molecules are aligned almost parallel to the surface similarly to the copper case. At the high exposure (60 langmuir), they are more tilted from the surface, but they are still largely (48 ± 5°) inclined from the surface normal as understood by a relatively small polarization dependence compared with that of the sanding-up phase on the Cu surfaces (see Figure 1). Further exposure induced no changes, indicating that this phase is a kinetically saturated phase. Immersion of a clean Ag substrate into an ethanolic solution of C6-thiol for a prolonged time gives rise to formation of a thermodynamically saturated monolayer. Polarization dependence of C K-edge NEXAFS spectra for the monolayers prepared on the Ag(111) and Ag(100) surfaces by

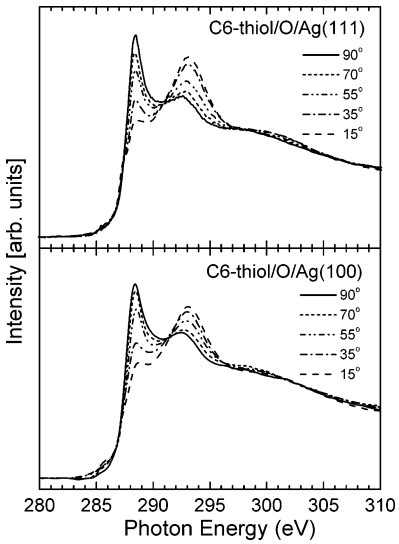

Figure 5. C K-edge NEXAFS spectra of C6-thiolate monolayers adsorbed on oxygen-covered Ag(111) (upper) and Ag(100) (lower) surfaces. These monolayers were prepared by immersion of the substrates into 1 mM ethanolic solution of C6-thiol for 48 h.

the immersion method are depicted in Figure 5. Since X-ray photoelectron spectroscopy revealed that the surfaces of these substrates were covered by a thin (approximately 1−2 ML) layer of oxygen,[9] these C6-thiolate monolayers are regarded as those formed on oxygen-covered Ag(111) and Ag(100) surfaces. Molecular oxygen in air can be adsorbed on the clean Ag surfaces during transfer from the UHV chamber to the solution (30 s). The C6-thiolate monolayers on the O/Ag(111) and O/Ag-(100) surfaces exhibit significant polarization dependence, meaning that a standing-up phase is formed. The average orientation angles of the molecular axes are estimated to be 17 $\pm$ 5° for O/Ag(111) and 19 $\pm$ 5° for O/Ag(100). From the edge-jump height, the molecular density of the immersed samples are estimated to be obviously higher than that prepared on the clean Ag(100) surface by the vacuum-deposition method: If the density of the immersed sample on O/Ag(100) is defined as 1, that for the vacuum-deposited sample is 0.7 at 60 langmuirs and 0.2 at 1 langmuir. Quantitative analyses indicated that the molecular axes in the vacuum-deposited sample (60 langmuirs) is tilted by 48 $\pm$ 5° from the surface normal. This significant increase in the tilt angle for the vacuum-deposited sample can be correlated to the reduction of the molecular density, caused by kinetic hindrance under the condition used here.

Si(111)-7 × 7. Clean Si(111) surfaces have dangling bonds which are highly reactive and can form covalent bonds with various adsorbates. Since hydrogen atoms are bound to the Si(111) surface at room temperature, atomic hydrogen generated by dissociative adsorption of thiols remains on the surface. In Figure 6 is shown the polarization dependence of C K-edge NEXAFS spectra for a saturated monolayer of C6-thiol on the Si(111)-7 × 7 surface taken at 300 K (upper) and 200 K (lower). The polarization dependence emerges a little at 200 K, but it disappears at 300 K. This temperature effect can be explained by thermal fluctuation of the molecular orientation. The presence of the thermal fluctuation is associated with a low molecular density. Since hydrogen atoms dissociated from thiols block half of the available adsorption sites for thiols, the molecular density cannot be so high. This is also confirmed by the experiment of C K-edge NEXAFS from CH_3SH and CH_3SSCH_3 on Si(111)-7 × 7, as shown in Figure 7. Both of the molecules were saturated on the Si(111) surface at room temperature. Since CH_3SSCH_3 is expected to adsorb dissociatively on the surface

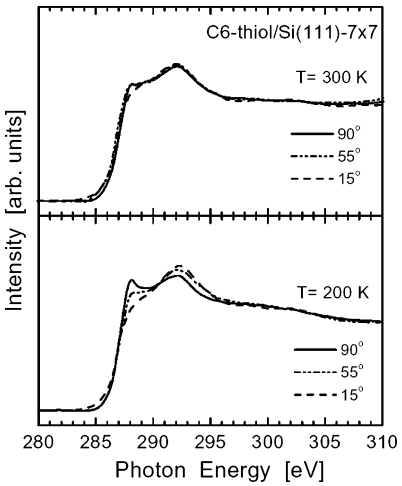

Figure 6. C K-edge NEXAFS spectra of a C6-thiolate saturated monolayer on a clean Si(111) −7 × 7 surface taken at 300 K (upper) and 200 K(lower).

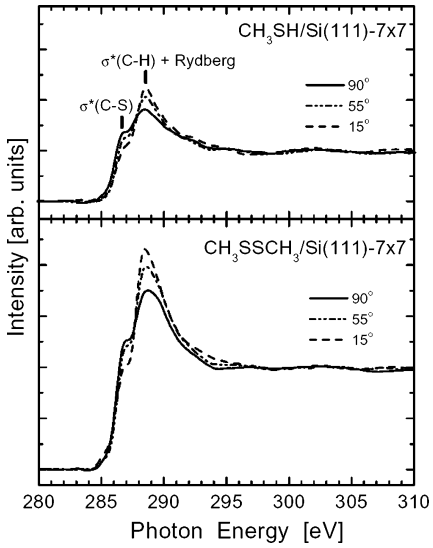

Figure 7. C K-edge NEXAFS spectra of methanethiol (CH_3SH) (upper) and dimethyl disulfide (CH_3SSCH_3) (lower) adsorbed on a clean Si(111)-7 × 7 surface at room temperature.

yielding two CH_3Ss, no site blocking by hydrogen should take place. The adsorption density of the CH_3S monolayer prepared from CH_3SSCH_3 is two times higher than that from CH_3SH as deduced from the edge-jump height. Similar spectral profiles for both of the monolayers indicate that the carbon moiety of the arriving molecules adsorbs as CH_3S with similar local electronic and geometric structures. Two features are observed in the NEXAFS spectra: a shoulder structure at 286.5 eV and a prominent peak at 288.5 eV. These features are assigned to C1s→σ*(C−S) and C1s→σ*(C−H) + Rydberg, respectively. From the polarization dependence of the σ*(C−S) shoulder, it is inferred that the S−C bond is inclined by 60 $\pm$ 15° from the surface normal. The orientation of the S−C bond shows little change irrespective of the CH_3S density and of the coadsorption with atomic hydrogen.

B. S K-Edge NEXAFS. S K-edge NEXAFS spectra provide information on the S−C bond orientation and the local electronic structure at the S-substrate interface. Figure 8 shows polarization dependence of S−K NEXAFS spectra taken for the saturated monolayer on Cu(111) and their curve-fitting results. A peak observed at 2473.2 eV is enhanced in the grazing-incidence spectrum (bottom) and reduces at the normal incidence (top).

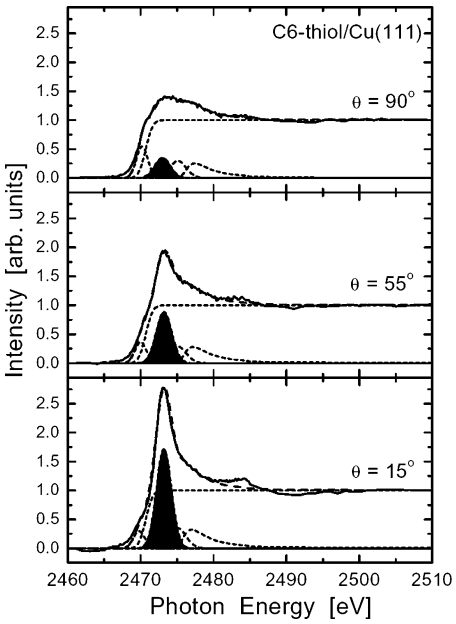

Figure 8. S K-edge NEXAFS spectra of a C6-thiolate saturated monolayer on Cu(111) and results of curve fitting using four Gaussian functions and a step function. Polarization dependence of a peak at 2473 eV (filled by black), which is assigned to the S 1s→σ*(S−C) transition, is used for estimation of the S−C bond angle.

This peak is assigned to the excitation from S 1s to σ*(S−C) whose transition moment directs along the S−C bond axis. From the polarization dependent intensity change, the S−C bond angle is estimated to be 32 ± 5°. A preedge peak at 2470.8 eV exhibits opposite polarization dependence; it is most enhanced at the normal incidence. A similar peak has been also observed for a saturated monolayer of C6-thiolate on Cu(100) and attributed to S1s→ π*(S−C).[9,11] As for higher-energy structures above 2475 eV, their origin has been still unclear. A saturated monolayer of C6-thiolate on an oxygen-covered Cu(100) surface with the (2$\sqrt{2}$ × $\sqrt{2}$)R45° LEED pattern[25] gives similar S−K NEXAFS spectra as shown in Figure 9. The (2$\sqrt{2}$ × $\sqrt{2}$)R45°-O/Cu(100) structure is a missing-row-type reconstruction with an oxygen coverage of 1/2 ML.[21] The saturated coverage of C6-thiolate on the surface is as much as 92% of that on the clean Cu(100). The S−C bond orientation is determined from the polarization dependence of the S−K NEXAFS spectra to be 41 ± 5° from the surface normal, which is more tilted compared to that on the clean Cu(100) (19 ± 10°).[11]

Figure 10 shows S−K NEXAFS spectra taken for saturated C6-thiolate monolayers prepared on O/Ag(111). Two prominent structures assigned to 1s → π*(S−C) and 1s → σ*(S−C) and a high-energy shoulder are observed at the edge region. Very similar results were obtained for O/Ag(100). From the polarization dependence of the σ*(S−C) peak, the S−C bond directions were estimated to be 37 ± 5° for O/Ag(111) and 39 ± 5° for O/Ag(100). The S−C bond in the kinetically saturated C6-thiolate monolayer on Ag(100) is tilted by 43 ± 10°,[9] which is almost the same as O/Ag(100). Since the molecular density of the saturated monolayer on O/Ag(100) is much higher than that on Ag(100), the molecular density is not a dominant factor to determine the S−C bond orientation.

C. S K-Edge SEXAFS. Oxygen atoms adsorbed on Cu(100) form a well-ordered structure with the commensurate (2$\sqrt{2}$ × $\sqrt{2}$)R45° periodicity as mentioned above. Thus, we performed S K-edge SEXAFS measurements for a C6-thiolate monolayer on (2$\sqrt{2}$ × $\sqrt{2}$)R45°-O/Cu(100) to study how C6-thiolate molecules are bound to the oxygen-covered reconstructed

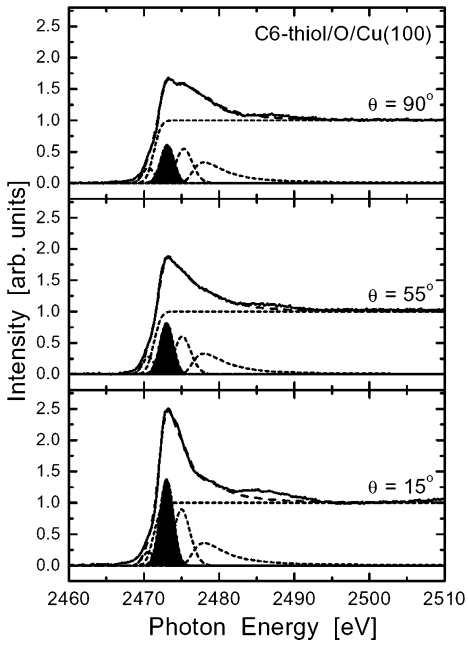

Figure 9. S K-edge NEXAFS spectra of a C6-thiolate saturated monolayer on an oxygen-covered Cu(100) surface and their curve-fitting results.

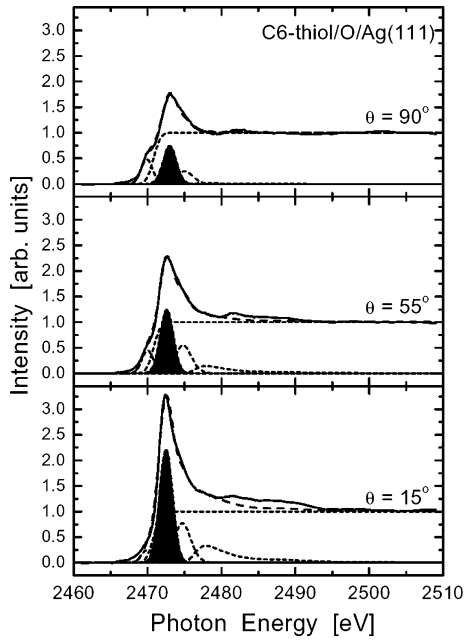

Figure 10. S K-edge NEXAFS spectra of a C6-thiolate saturated monolayer on an oxygen-covered Ag(111) surface and their curve-fitting results.

surface. The k^2-weighted EXAFS oscillation function $k^2\chi(k)$ were obtained by means of the standard analysis procedures: preedge and postedge subtraction and normalization with the atomic absorption coefficients.[26,27] Figure 11a shows resultant $k^2\chi(k)$ functions for the C6-thiolate monolayer on (2$\sqrt{2}$ × $\sqrt{2}$)-R45°-O/Cu(100) taken at the normal (90°) and the grazing incidence (15°). The oscillation amplitude is much less than that for the clean Cu(100) despite a similar molecular density, suggesting significant static disorder at the S+O/Cu(100) interface. The corresponding Fourier transforms (Δk=3.0−10.6 Å^{-1}) are shown in Figure 11b. In the normal-incidence curve, a prominent peak is observed at around 2.0 Å, which is attributed to the contribution from the S−Cu(1) shell. Above 3 Å, an apparent peak is appreciable at 3.4 Å. A plausible assignment

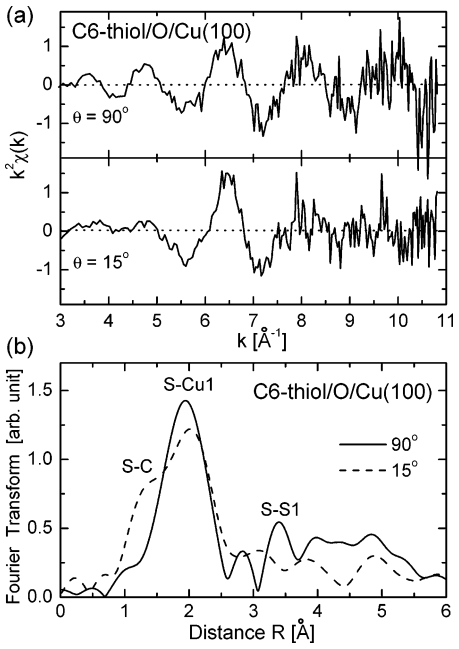

Figure 11. (a) S K-edge k^2-weighted EXAFS oscillation function $k^2\chi(k)$ taken for a C6-thiolate saturated monolayer on an oxygen-precovered Cu(100) surface. The precovered oxygen overlayer formed a $(2\sqrt{2}\times\sqrt{2})$R45° structure with a coverage of 0.5 ML. Polarization dependence was investigated with two X-ray incident angles of 90° and 15° from the surface parallel. (b) Fourier transforms of the EXAFS oscillation function $k^2\chi(k)$.

TABLE 1: Effective Coordination Numbers and Their Ratio for the S−Cu(1) Shell[a]

	N (90°)	*N* (15°)	*N* (90°)/ *N*(15°)
atop	0	2.72	0
bridge	0.96	3.78	0.26
hollow	3.85	4.26	0.90
deep-hollow[b]	4.11	3.80	1.09
exp.	3.8 ± 0.4	3.5 ± 0.4	1.09 ± 0.15

[a] The experimental results are compared with calculated values for the sulfur atom at high-symmetry sites of the unreconstructed Cu(100) substrate except for *b* with the S−Cu(1) distance of 2.26 Å. [b] Four-fold hollow site with a substrate reconstruction where the Cu atoms directly bonding to the sulfur atom are laterally displaced outward by 0.06 Å from the regular position of the unreconstructed surface.

of this peak is scattering from the nearest sulfur atoms located at adjacent hollow site along [110] direction as discussed below. In the grazing-incidence curve, the S−C shell contribution is seen as a shoulder structure at around 1.3 Å and the S−Cu(1) shell appears at around 2.0 Å with a little less intensity.

To determine the adsorption site, we analyzed polarization dependence of the effective coordination number for the S−Cu-(1) shell using $\chi(k)$ of a CH_3S/Cu(100) system[28] as the standard, where the coordination number and the S−Cu(1) distance are $N = 4$ and $R = 2.29$ Å, respectively. The results are compared with calculated values for high-symmetry sites of the unreconstructed and reconstructed surfaces as listed in Table 1. Obviously, the experimental coordination number ratio is not consistent with any high-symmetry site of the unreconstructed surface. Since the experimental result is beyond the value for the highest coordination site (hollow site), the sulfur atoms should be located at a deep hollow site where the Cu(1) atoms are displaced outward from the regular positions of the unreconstructed surface. To reproduce the experimental coordination numbers and their ratio, an outward displacement of the Cu atoms by 0.06 Å is needed as shown in Table 1. According to the literature,[21] the $(2\sqrt{2} \times \sqrt{2})$R45°-O/Cu(100) surface exhibits a missing-row reconstruction where the Cu atoms next to the missing row are laterally displaced by 0.3 Å toward the missing row as schematically illustrated in Figure 12a. Thus, if we consider the $(2\sqrt{2} \times \sqrt{2})$R45°-O/Cu(100) surface as the starting point, the C6-thiolate adsorption induces a redisplacement of the first-layer Cu atoms toward the sulfur atom by approximately 0.25 Å as indicated by thick arrows in Figure 12a.

TABLE 2: The Structural Parameters for the Local Structure around the Sulfur Atom Determined from S K-Edge SEXAFS

	O/Cu(100)	Cu(100)[a]
R(S-C) [Å]	1.81 ± 0.04	1.82 ± 0.04
R(S-Cu(1)) [Å]	2.26 ± 0.02	2.28 ± 0.02
R(S-S(1)) [Å]	3.74 ± 0.05[b]	3.66 ± 0.05

[a] Reference 11. [b] This distance is in good agreement with the calculated S−S(1) distance based on the expanded hollow site shown in Table 1 (3.75 Å).

Curve-fitting analyses in *k*-space were carried out after Fourier filtering of the contribution of interest: S−C(ΔR = 0.8−1.3 Å), S−Cu(1)(ΔR = 1.4−2.5 Å), and S−S(1)(ΔR = 3.1−3.6 Å) shells. The structural parameters around the sulfur atom were determined as listed in Table 2. The R(S−C) and the R(S−Cu(1)) values coincided with those on the clean Cu(100) within the errors, indicating that the local structure around the sulfur atom is almost the same despite the presence of oxygen atoms. The local structure is schematically illustrated in Figure 12b. The distance to the nearest sulfur atoms R(S−S(1)) is a little longer than that on the clean Cu(100) probably because the nearest Cu(1) atoms are slightly expanded from the regular position of the unreconstructed Cu(100) surface. Considering the expansion of the Cu(1) atoms yields a S−S(1) distance of 3.75 Å, which is consistent with the observed distance (3.74 ± 0.05 Å).

IV. Discussion

A. Role of Precovered Oxygen to Self-Assembly. Surface oxygen atoms promote the dissociation of hydrogen-containing bonds such as O−H and N−H. For example, ammonia (NH_3) molecules dissociatively adsorb on an oxygen-adsorbed Ni(110) surface at room temperature to yield NH_2 and OH,[29] while they molecularly adsorb on a clean Ni(110) and desorb without dissociation.[30] The surface OH species produced by hydrogen abstraction desorbs as H_2O via disproportional reaction ($2OH_a \rightarrow O_a + H_2O_g\uparrow$).[29] Methanol ($CH_3OH$) adsorption on Cu(110) shows a similar behavior; preadsorbed oxygen atoms induce the formation of surface methoxy (CH_3O) and gaseous H_2O at room temperature following the reaction scheme ($2CH_3OH_a + O_a \rightarrow 2CH_3O_a + H_2O_g\uparrow$).[31] The enhanced adsorption rate of C6-thiol on the O/Cu(111) surface is similarly ascribed to hydrogen abstraction from the S−H bond by the preadsorbed oxygen atoms. The oxygen-assisted adsorption is supported by the stoichiometric removal of the surface oxygen. The enhanced adsorption of alkanethiols on surface oxygen has been also found for Au and Ag surfaces.[8,32]

Since short alkanethiols such as C6-thiol are not bound to solid substrates in the form of thiol at room temperature, the S−H bond scissoring is the key process for adsorption. The promotion effect of the surface oxygen on the thiol adsorption is considered to have twofold mechanisms: (1) abstraction of H by the "active" oxygen atom and (2) enhanced dissociation of the S−H bond by the oxygen-modified metal atoms. The former mechanism has been proposed for the N−H dissociation

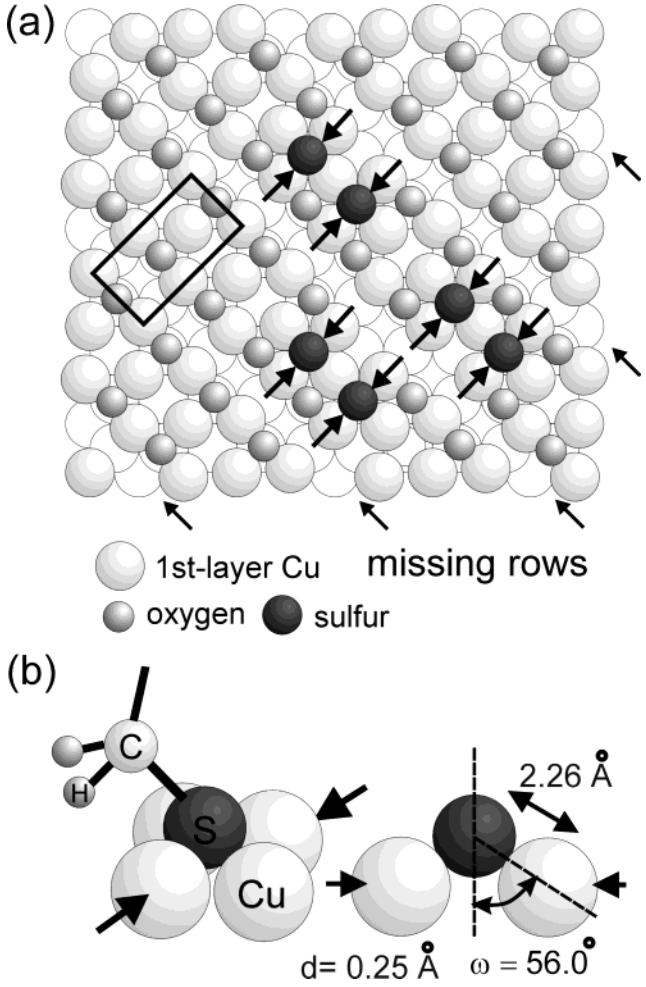

Figure 12. (a) Structural model for adsorption site of the sulfur atoms of the C6-thiolate molecules on a $(2\sqrt{2}\times\sqrt{2})$R45°-O/Cu(100) surface. The $(2\sqrt{2}\times\sqrt{2})$R45°-O surface shows a missing-row reconstruction, where every fourth oxygen row along the ⟨001⟩ direction is removed (indicated by thin arrows) and the remaining rows are laterally shifted toward the missing rows. The sulfur atoms occupy deep fourfold hollow sites with a lateral displacement of Cu atoms toward the sulfur atom (indicated by thick arrows). Surface oxygen atoms are partially removed probably because of formation and desorption of H_2O with hydrogen atoms originating from the S−H headgroups. (b) Geometrical structure around the sulfur atom obtained from curve-fitting analyses of the EXAFS oscillations. Although the first-coordination Cu atoms are laterally shifted by 0.25 Å toward the sulfur atom, there still remains a lateral expansion of Cu atoms by 0.06 Å with respect to the regular position of the unreconstructed Cu(100) surface.

in the NH_3/O/Ni(110) system because the dissociation was observed by the atom-resolved STM technique to take place at a specific oxygen site, which is the end of one-dimensional (1D) −O−M−O− chains. Since this oxygen atom is not fully coordinated, it is chemically active enough to abstract hydrogen from arriving molecules. A similar site-specific dissociation was observed for the O−H bond of methanol on an O/Cu(110) surface.[31] Since the O−H bond energy is higher than the S−H one, this mechanism might operate also for the thiol adsorption.[33] As for the latter mechanism, oxygen-induced changes in the thiol−metal interaction are important to the dissociation. An X-ray standing wave study of methanethiol (CH_3SH) adsorbed on a clean Cu(111) revealed that it prefers the atop site at low temperature but decomposes into CH_3S and H with increasing temperature.[34] According to density functional theory (DFT) calculations for CH_3SH adsorbed on Au(111),[35] the thiol is adsorbed at the atop site with the sulfur atom. Molecular orbital calculations for H_2S adsorbed on Au(111) showed that H_2S also bonds to the atop site through a σ-bond mainly composed of the sulfur p-orbitals and the gold 6s orbital.[36] Since this S−Au bonding orbital corresponds to the lowest unoccupied molecular orbital (LUMO) of H_2S that has an antibonding character with respect to the S−H bond,[37] the bonding to the metal surface weakens the S−H bond strength. Thus, the electron donation from the substrate to the antibonding LUMO is a cause of the dissociation. The filled d bands of the coinage-metal surfaces are shifted up toward the Fermi level by the interaction with the lower-lying oxygen 2p levels. The increased density of states near the Fermi level originating from the upshift of the d band can contribute to the donation to the LUMO of thiols, which may result in the enhanced dissociation.

To understand the interface structure of thiol/oxygen-covered metal surface, we performed S−K SEXAFS study on the C6-thiol/$(2\sqrt{2}\times\sqrt{2})$R45°-O/Cu(100) system as mentioned above. The obtained local structure around the sulfur atom is almost the same as that on a clean Cu(100) except for a slight lateral expansion (0.06 Å) of the Cu atoms that directly bond to the sulfur atom. The $(2\sqrt{2}\times\sqrt{2})$R45°−O structure consists of an array of one-dimensional (1D) −O−Cu−O− chains as shown in Figure 12a. The thiol adsorption causes the removal of the oxygen atoms via water formation reaction and destroys the 1D −O−Cu−O− chains by the stronger S−Cu interactions.

B. Effects of Substrates on Self-Assembled Structure. We studied systematically both alkyl-chain angles and S−C bond angles in the hexanethiolate SAMs on the various substrates. The obtained results are summarized together with those for related SAM systems in Table 3. Although the alkyl chains always adopt flat-lying configuration at low coverages irrespective of substrate, the orientations of the alkyl chain and of the S−C bond change at the saturation coverage strongly depending on the substrate. To examine the correlation of the orientation between the alkyl chain and the S−C bond, we plot the alkyl orientation angle versus the S−C orientation angle for each substrate as shown in Figure 13a. No apparent correlation is discernible from the plot. Similar S−C bond angles do not necessarily cause similar alkyl orientation angles, which means that the rotation angle about the alkyl-chain axis varies significantly depending on the chemical environment in the SAMs. Thus, the S−C bond angle at the molecule−substrate interface is not a decisive factor to the alkyl-chain orientation.

The molecular densities of the saturated SAMs were estimated from the edge-jump height and are listed in the right column of Table 3, as the "molecular area", which corresponds to the surface area for one molecular occupation. Figure 13b shows the change of alkyl orientation angle as a function of molecular area. As the molecular area increases, the alkyl chains get more tilted from the surface normal. The data points are almost in accordance with a simple curve $\theta = \cos^{-1}(A/A_0)$, where A_0 is the molecular area in the vertically aligned alkyl chains and A is the one in the actual SAM. This agreement indicates that primarily the molecular density controls the chain orientation in the alkanethiolate SAMs.

The self-assembly of thiols on the metal substrates can be divided into two major processes: (1) chemisorption via S−H dissociation and (2) two-dimensional (2D) arrangement via surface diffusion. In long-chain thiols, stretching of entangled alkyl chains is an additional important process occurring at the final stage.[4] The dissociation of the S−H bond strongly depends on the electronic structure of the surface as mentioned above. The dissociation ability of the surface influences the saturated molecular density. In fact, the oxygen-precovered Ag surfaces

TABLE 3: Adsorption Structure and Surface Density of Hexanethiolate Adsorbed on Various Substrates

	low coverage	saturation coverage		
substrate	orientation of alkyl chain	alkyl-chain angle from the surface normal	S−C bond angle from the surface normal	molecular area [Å^2/molecule]
Au(111)	flat-lying	35 ± 5°[a]	(∼50°)[b,e]	21.6
Ag(100)	flat-lying	48 ± 5°	43 ± 10°[c]	25 ± 2
O/Ag(111)		17 ± 5°	38 ± 5°	18 ± 1
O/Ag(100)		19 ± 5°	37 ± 5°	18 ± 1
Cu(111)	flat-lying	30 ± 5°	32 ± 5°	19.7
Cu(100)[d]	flat-lying	27 ± 5°	19 ± 10°	19.7
O/Cu(111)	flat-lying	38 ± 5°		23 ± 1
O/Cu(100)			41 ± 5°	24 ± 1
Si(111)		49 ± 5°	(60 ± 10°)[e]	62 ± 5

[a] Reference 20. [b] Reference 38. [c] Reference 9. [d] Reference 11. [e] Parentheses: S−C bond angle obtained for methylthiolate monolayers.

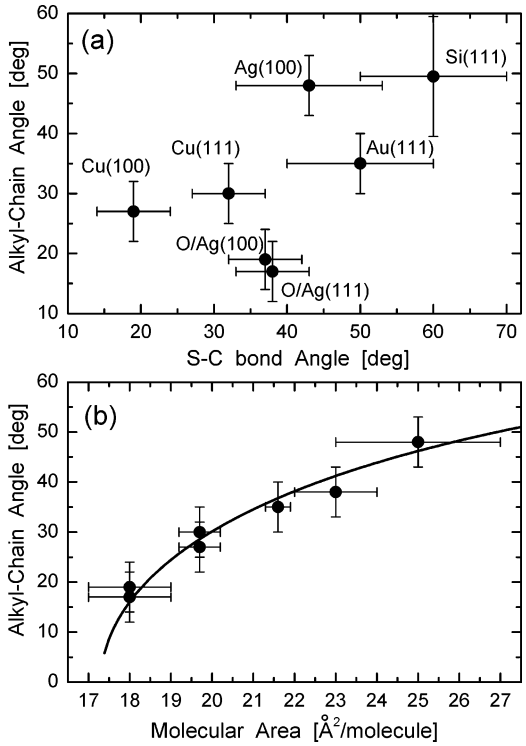

Figure 13. (a) Correlation between S−C bond and alkyl-chain angles. (b) Plot of alkyl-chain angles as a function of molecular area (effective surface area that one molecule occupies in the SAM). Thick line indicates a simple relation between the alkyl-chain angle and the molecular area, $\theta = \cos^{-1}(A/A_0)$, where A_0 is the molecular area in the vertically aligned alkyl chains and A is the one in the actual SAM.

can adsorb approximately 1.4 times more alkanethiol molecules compared with the clean Ag surface. A similar trend has been also observed for oxidized and clean Au surfaces.[32] In Cu, however, the saturated molecular density is lower for the oxygen-precovered surface. This is probably because the oxygen-induced restructuring of the Cu surface reduces available sites for thiolate adsorption as shown in Figure 12a. The Si(111)-7 × 7 surface is exceptional, since the site-blocking by dissociated hydrogen atoms and the limited site density available for adsorption considerably decreases the saturated coverage despite facile dissociation of the S−H bond by the dangling bond. Thus, the substrate plays a decisive role to the saturated chemisorption density and consequently determines the chain orientation. Then, the adsorbed thiolates diffuse on the surface and pack into an energetically favorable 2D arrangement. The balance between the intermolecular interactions and the molecule−substrate interfacial energy due to corrugation of the surface potential is important to the arrangement. During this process, the internal degrees of freedom of the molecule such as rotation about the molecular axis play an important role to stabilize the total energy of the SAM system.

V. Conclusions

We have studied substrate dependence of alkyl-chain and S−C bond orientations in C6-thiolate SAMs by using C−K and S−K NEXAFS spectroscopy. There is no straightforward correlation found between the alkyl-chain and the S−C bond orientations. The alkyl-chain orientation is primarily correlated with the molecular density irrespective of substrate surface. Surface oxygen atoms adsorbed on Cu and Ag surfaces promote C6-thiol adsorption via enhanced S−H bond dissociation. A part of the surface oxygen atoms are removed by the thiol adsorption as H_2O. The adsorption structure of C6-thiolate molecules on an oxygen-saturated Cu surface has been investigated by the S−K SEXAFS technique. Detailed analyses of the SEXAFS data revealed that the C6-thiol adsorption induces displacement of surface Cu atoms toward the sulfur atom of the thiolate to form an energetically favorable (deep) fourfold hollow site. The local structure around the sulfur atom of the thiolate adsorbed on the oxygen-covered Cu surface is close to that on the clean Cu surface.

Acknowledgment. The authors are grateful for the financial support of the Ministry of Education, Sports, and Culture (Grant No.11640576, 15350008). This research was performed under the approval of the Photon Factory Program Advisory Committee (PF-PAC 1999G078, 2001G305). H. K. acknowledges financial support from the Toyota Physical and Chemical Research Institute.

References and Notes

(1) Dubois, L. H.; Nuzzo, R. G. *Annu. Rev. Phys. Chem.* **1992**, *43*, 437.
(2) Ulman, A. *Chem. Rev.* **1996**, *96*, 1533.
(3) Poirier, G. E. *Chem. Rev.* **1997**, *97*, 1117.
(4) Schreiber, F. *Prog. Surf. Sci.* **2000**, *65*, 151.
(5) Heinz, R.; Rabe, J. P. *Langmuir* **1995**, *11*, 506.
(6) Fenter, P.; Eisenberger, P.; Li, J.; Camillone, N., III; Bernasek, S.; Scoles, G.; Ramanarayanan, T. A.; Liang, K. S. *Langmuir* **1991**, *7*, 2013.
(7) Laibinis, P. E.; Whitesides, G. M.; Allara, D. L.; Tao, Y.-T.; Parikh, A. N.; Nuzzo, R. G. *J. Am. Chem. Soc.* **1991**, *113*, 7152.
(8) Himmelhaus, M.; Gauss, I.; Buck, M.; Eisert, F.; Wöll, Ch.; Grunze, M. *J. Electron Spectrosc. Relat. Phenom.* **1998**, *92*, 139.
(9) Kondoh, H.; Tsukabayashi, H.; Yokoyama, T.; Ohta, T. *Surf. Sci.* **2001**, *489*, 20.
(10) Imanishi, A.; Isawa, K.; Matsui, F.; Tsuduki, T.; Yokoyama, T.; Kondoh, H.; Kitajima, Y.; Ohta, T. *Surf. Sci.* **1998**, *407*, 282.
(11) Kondoh, H.; Saito, N.; Matsui, F.; Yokoyama, T.; Ohta, T.; Kuroda, H. *J. Phys. Chem. B* **2001**, *105*, 12870.
(12) Driver, S. M.; Woodruff, D. P. *Surf. Sci.* **2000**, *457*, 11.
(13) Zharnikov, M.; Frey, S.; Rong, H.; Yang, Y.-J.; Heister, K.; Buck, M.; Grunze, M. *Phys. Chem. Chem. Phys.* **2000**, *2*, 3359. Rong, H.-T.; Frey,

S.; Yang, Y.-J.; Zharnikov, M.; Buck, M.; Wühn, M.; Wöll, Ch.; Helmchen, G. *Langmuir* **2001**, *17*, 1582.

(14) Ishizaka, A.; Shiraki, Y. *J. Electrochem. Soc.* **1990**, *133*, 233.

(15) In Cu surfaces, partial dissociation of adsorbed thiolates into sulfide and alkyl chain becomes nonnegligible at elevated temperatures higher than ca. 310 K. The temperature of the Cu surfaces was kept lower than 290 K during and after C6-thiol exposure.

(16) Namba, H.; Daimon, H.; Idei, Y.; Kosugi, N.; Kuroda, H.; Taniguchi, M.; Suga, S.; Murata, Y.; Ueyama, K.; Miyahara, T. *Rev. Sci. Instrum.* **1989**, *60*, 1909.

(17) Ohta, T.; Stefan, P. M.; Nomura, M.; Sekiyama, H. *Nucl. Instrum. Methods A* **1986**, *246*, 373. Kitajima, Y. *J. Electron Spectrosc. Relat. Phenom.* **1996**, *80*, 405.

(18) Väterlein, P.; Fink, R.; Umbach, E.; Wurth, W. *J. Chem. Phys.* **1998**, *108*, 3313.

(19) Kondoh, H.; Kodama, C.; Sumida, H.; Nozoye, H. *J. Chem. Phys.* **1999**, *111*, 1175.

(20) Kondoh, H.; Matsui, F.; Ehara, Y.; Yokoyama, T.; Ohta, T. *Lamgmuir* **2001**, *17*, 8178.

(21) Besenbacher, F.; Nørskov, J. K. *Prog. Surf. Sci.* **1993**, *44*, 5.

(22) Schmidt, E.; Schurig, W.; Sellschopp, W. *Technol. Mech. Termodyn.* **1930**, *1*, 53.

(23) Bagus, P. S.; Weiss, K.; Shertel, A.; Wöll, Ch.; Bruun, W.; Hellwig, C.; Jung, C. *Chem. Phys. Lett.* **1996**, *248*, 129.

(24) Väterlein, P.; Fink, R.; Umbach, E.; Wurth, W. *J Chem. Phys.* **1998**, *108*, 3313.

(25) Zeng, H. C.; McFarlane, R. A.; Mitchell, K. A. R. *Surf. Sci.* **1989**, *208*, L7.

(26) *X-ray Absorption: Principles, Applications, Techniques of EXAFS, SEXAFS and XANES*; Koningsberger, D. C., Prins, R., Eds.; Wiley: New York, 1988.

(27) Yokoyama, T.; Hamamatsu, H.; Ohta, T. *EXAFSH*, version 2.1, The University of Tokyo, 1993.

(28) Imanishi, A.; Takenaka, S.; Yokoyama, T.; Kitajima, Y.; Ohta, T. *J. Phys. (Paris)* **1997**, IV7−C2, 701.

(29) Ruan, L.; Stensgaard, I.; Lægsgaard, E.; Besebbacher, F. *Surf. Sci.* **1994**, *314*, L873.

(30) Klauber, C.; Alvey, M. D.; Yates, J. T., Jr. *Surf. Sci.* **1985**, *154*, 139.

(31) Francis, S. M.; Leibsle, F. M.; Haq, S.; Xiang, N.; Bowker, M. *Surf. Sci.* **1994**, *315*, 284.

(32) Yan, C.; Gölzhäuser, A.; Grunze, M.; Wöll, Ch. *Langmuir* **1999**, *15*, 2414.

(33) The O−H bond energy in H_2O is 459 kJ/mol, while the S−H one in H_2S is 364 kJ/mol. *J. Chem. Thermodyn.* **1978**, *10*, 903.

(34) Jackson, G. J.; Woodruff, D. P.; Jones, R. G.; Singh, N. K.; Chan, A. S. Y.; Cowie, B. C. C.; Formoso, V. *Phys. Rev. Lett.* **2000**, *84*, 119.

(35) Grönbeck, H.; Curioni, A.; Andreoni, W. *J. Am. Chem. Soc.* **2000**, *122*, 3839.

(36) Sellers, H. *Surf. Sci.* **1993**, *294*, 99.

(37) Sellers, H.; Ulman, A.; Shnidman, Y.; Eilers, J. E. *J. Am. Chem. Soc.* **1993**, *115*, 9389.

(38) Kondoh, H.; Iwasaki, M.; Shimada, T.; Amemiya, K.; Yokoyama, T.; Ohta, T.; Shimomura, M.; Kono, S. *Phys Rev. Lett.* **2003**, *90*, 066102.